Progress In Electromagnetics Research C, Vol. 50, 155–164, 2014

Double-layered Circular Microstrip Reflectarray Element with Broad Phase Range

Wai-Hau Ng[1], Eng-Hock Lim[1, *], Fook-Loong Lo[1], and Kia-Hock Tan[2]

Abstract—In this paper, a double-layered microstrip reflectarray element is studied. The unit element consists of a circular patch sandwiched between two substrates and a cross-slotted circular patch placed on the top-most surface. The radii of the two circular patches as well as the cross-slot lengths are varied simultaneously for controlling the phase range and the gradient of the reflection phase angle. Study shows that the sensitivity of the reflection phase angle can be made slower by utilizing substrates with lower dielectric constants. The component performance is studied using a rectangular waveguide and good agreement is found between the simulation and experiment. A wide reflection phase range of 681.82° with loss magnitude less than -1 dB is achievable in the reflection phase angle. A complete parametric analysis has been conducted to study the reflection characteristics of the proposed reflectarray unit element.

1. INTRODUCTION

Parabolic dish and phased array are among the most popular antennas used by various wireless applications. However, the curvature surface of the parabolic antenna has made the manufacturing process difficult and the hardware itself very bulky. For a phased array, many power dividers are usually needed to provide phase shifts, which can be lossy in the high frequency ranges [1]. In 1963, Berry et al. came up with the earliest concept of reflectarray which was built by cascading the radiating apertures of multiple truncated waveguides [2]. This structure was bulky, and as a result, Berry's invention had not been popular until the introduction of microstrip reflectarrays by Huang in 1991 [3]. A microstrip reflectarray is a thin flat plate structure which consists of many microstrip resonators or guided elements printed on a grounded substrate. It has many advantages such as low profile, flat surface, and low manufacturing costs [3, 4]. When used for designing reflectarray, a microstrip unit element is always required to provide low reflection loss, large reflection phase range, and slow phase change in the reflection phase angle.

Since then, various resonating and guided elements with different phasing schemes such as variable-size resonators [4–6], phase-delay stubs [7–9], rotated structures [10], and slotted grounds [11] have been deployed for introducing additional phase to the re-radiated wave beams. Varying element size is a conventional way for generating phase shift, but the separation distances between the neighboring elements can sometimes change very abruptly. Guiding wave into an attaching stub can also alter the phase of the scattered wave. Nevertheless, spurious radiation can be a problem when there is bending in the stub. Although rotating the angular orientation of the element is an easy phasing technique, it is more suitable for circular polarization. Creating slots beneath a microstrip resonator can introduce phase shift but it increases the antenna backlobe. In [12], a multilayer unit element with variable slot lengths etched on the ground plane is capable of providing a phase range of 330°. However, a phase range of less than 360° implies that such a unit element is not sufficient to be used for designing

Received 18 March 2014, Accepted 28 May 2014, Scheduled 5 June 2014

* Corresponding author: Eng Hock Lim (limeh@utar.edu.my).
[1] Department of Electrical and Electronic Engineering, Universiti Tunku Abdul Rahman, Kuala Lumpur, Malaysia. [2] Department of Industrial Engineering, Universiti Tunku Abdul Rahman, Kuala Lumpur, Malaysia.

large-size reflectarrays. It is always very desirable to obtain large reflection phase range and gradual phase slope. One of the efficient ways to generate broad phase range ($> 360°$) is to excite multiple resonances in an element or to combine the resonances of different elements. In [13], a fractal ring is incorporated with a square ring for generating reflectarray phase range of 700°. Florencio [14] has combined the resonances of three parallel printed dipoles to achieve a phase range of greater than 600° with linear phase slope. In [15–17], it was shown that different ring elements can be concentrically placed to provide large reflection phase range of exceeding 360°, yielding reasonable reflection phase slope. The main advantage of the unit elements in [13–17] is that all of them can be made on a single layer, with the price of larger footprint. Also, for the structures formed by concentric rings, the gap between the inner ring and the outer ring of the elements has to be made very narrow, usually less than 0.5 mm, making the fabrication process and alignment very difficult. Exploiting the parasitic elements of a multilayer mushroom structure has also been demonstrated to be a possible way to introduce reflection phase shift to an incoming wave [18, 19]. However, optimization of the reflection phase is greatly dependent on the parasitic capacitance and inductance which may involve massive calculations. The computational process has made the implementation extremely tedious. Later, in [20], the concept of fractal structures was applied for designing a unit element to mitigate mutual coupling effect between the reflectarray elements. Although reflection phase range of 700° was achievable, careful design was required as the structure was somewhat complex. To reduce the circuit footprint, effort has been made to stack elements using the multilayer structures [6]. In [21], a slot-coupled delay line and a variable-length slot are simultaneously used as the phase-shifting element of a multilayer patch to give a reflection phase range of more than 1000°. However, the delay line requires additional circuit size.

In this paper, the double-layered microstrip unit element is explored for reflectarray design. A cross-slotted circular microstrip patch is stacked on top of another solid circular patch for attaining a very broad phase range of 681.82° with low reflection loss. The element footprint is slightly more compact than that in [21] as it does not need additional space for loading line. The reflection characteristics are studied for different patch sizes, slot dimensions and substrate dielectric constants. CST Microwave Studio was used for all the simulations while R&S® ZVB8 Vector Network Analyzer (VNA) was deployed for experimental verification.

2. UNIT CELL CONFIGURATION

Figure 1 illustrates the schematic of the proposed microstrip double-layered reflectarray unit element, which is made on a Duroid RO4003C substrate with thickness of $h = 1.524\,\text{mm}$ and dielectric constant of $\varepsilon_r = 3.38$ and $\tan\delta = 0.027$. The top layer consists of a circular patch with radius R_1 laminated on Substrate 1. It is etched with a pair of rectangular slots with length of $L_1 = L_2$ and width of $W_1 = W_2 = 1.4\,\text{mm}$. The slots are placed concentrically at the center of the circular patch to form a cross as depicted in Figure 1(a). The two rectangular slots are designed in such the way that $L_1 = L_2 = 2 \times (R_1 - 0.5)$. With reference to Figure 1(b), the middle layer consists of a circular patch with radius of R_2 and it is sandwiched in between Substrate 1 and 2. A thin copper lamination which acts as the ground is placed on the bottom-most surface of the structure as shown in Figure 1(c). Figure 1(d) shows a photograph of the fabricated prototype.

The reflectarray unit element can be simulated using either the waveguide model or Floquet model. Figure 2(a) shows the boundary conditions for the waveguide model. With reference to the figure, the reflectarray unit element can be placed at bottom of the waveguide section, and a y-polarized wave (6.5 GHz) is generated from another end of the waveguide section, which is also the wave port. The wave propagates towards the direction of the unit element. All of the waveguide boundaries are defined as perfect electrical conductors (PEC). The illuminating angle (α) of the incident electromagnetic wave changes with respect to the operating frequency (f) and the waveguide cut-off frequency (f_c), which can be calculated using $\alpha = 90° - \cos^{-1}\sqrt{1 - (\frac{f_c}{f})^2}$. This angle is calculated to be $\alpha = 48.58°$ for the operating frequency of $f = 6.5\,\text{GHz}$. The main advantage of the waveguide model is that measurement can be easily performed on this unit element using a section of waveguide. However, the size of the unit element is restricted by the waveguide cross section ($a \times b$), making this method unsuitable for simulating element that has dimension larger than the waveguide. Figure 2(b) illustrates the boundary conditions of the Floquet model, where two of its boundaries are defined as perfect electrical conductors (PEC)

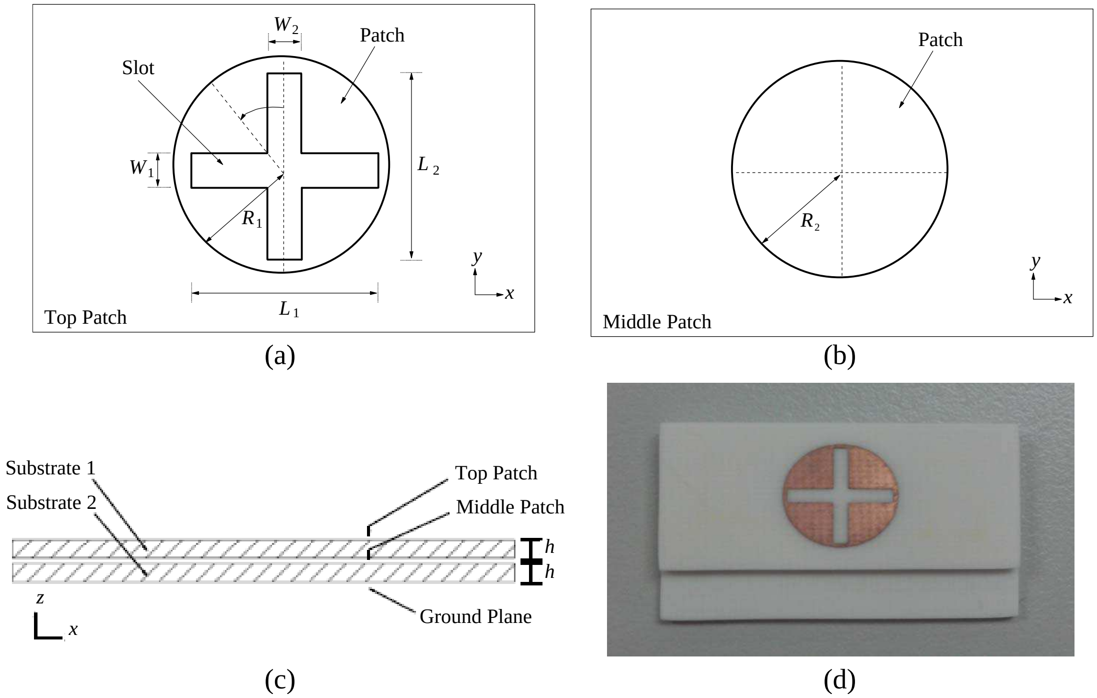

Figure 1. Double-layered microstrip reflectarray unit element. (a) Top patch. (b) Middle patch. (c) Side view. (d) Photograph of the fabricated prototype.

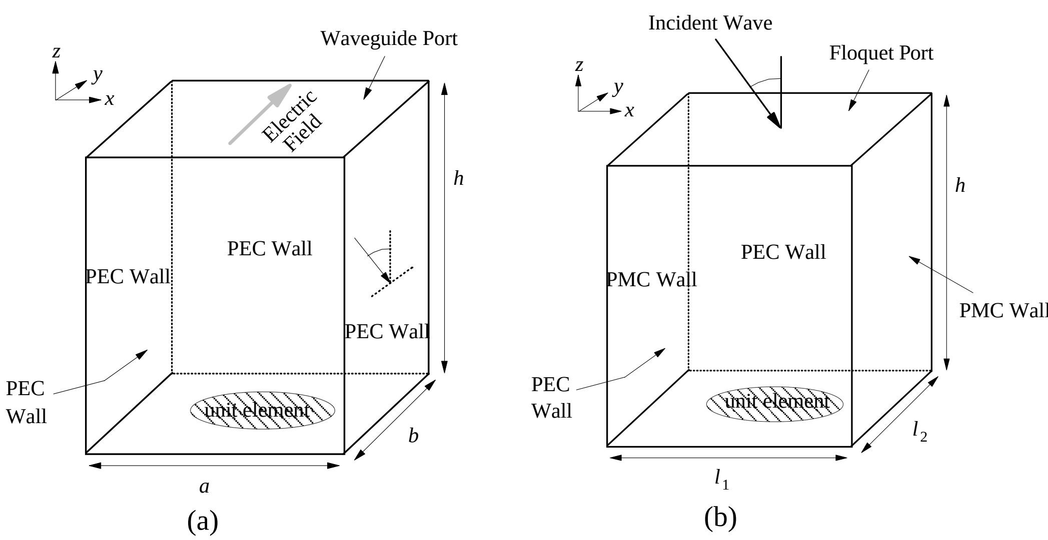

Figure 2. (a) Waveguide model. (b) Floquet model.

while the other two are defined as perfect magnetic conductors (PMC). Such boundary conditions have effectively expanded the element into a two-dimensional infinite array, with mutual coupling between the neighbouring elements considered [22]. Unlike the waveguide method, Floquet method can be used to simulate any unit element regardless of its size. Since the illuminating angle of the Floquet method is not restricted by the operating frequency, it gives much more freedom in choosing frequency and illuminating angle (θ) when designing a unit element. Also here, l_1 and l_2 can be made any values. The main disadvantage of the Floquet method is that a unit element that is simulated using this method

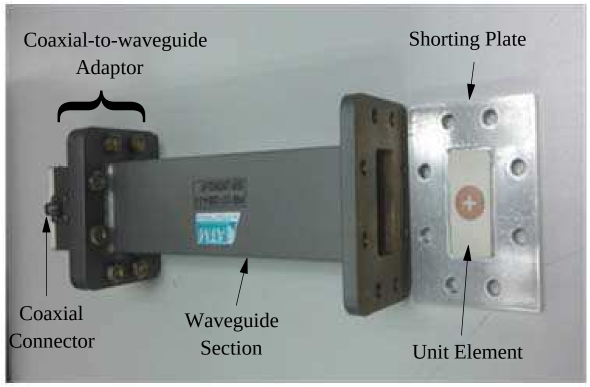

Figure 3. Experimental setup of the waveguide model.

cannot be verified experimentally at the element level.

In this paper, a waveguide working in the C-band (5.8 GHz–8.2 GHz), with dimension $a \times b \times h$ (34.85 mm $\times$ 15.8 mm $\times$ 154 mm), is used for experiment, shown in Figure 3. A coaxial-to-waveguide adaptor is used to connect the waveguide section to the port cable of a vector network analyzer (R&S® ZVB8, 300 kHz–8 GHz), which provides microwave source. The ATM rectangular horn (PNR 137-440-2, 5.8 GHz–8.2 GHz) can be used to feed the full-range reflectarray designed using this unit element. Nonetheless, feeding horn is not needed in this case since it only involves unit element. The calibration procedure will now be briefly described. First, the standard one-port OPEN-SHORT-LOAD calibration is performed on the output end of the port cable. In this case, the other end of the cable is connected to the output port of the vector network analyzer. The calibrated cable is then connected to the coaxial connector of the coaxial-to-waveguide adaptor. With the use of a flat shorting plate, de-embedding procedure is conducted so that the reference plane is moved flush to the adaptor flange, making it tally with the simulation setting. This was manually done by compensating additional length until the reflection phase is close to 180° in a particular frequency range, which simply implies that the reference plane is now aligned along the shorting plate. Finally, the unit element sample is carefully trimmed to make it fit into a rectangular trench with depth of $\sim$3 mm.

3. RESULTS AND DISCUSSION

Figure 4 depicts the measured and simulated reflection losses and reflection phase angles at the wave port when the patch radius $R_2 (= R_1)$ is varied from 1.5 to 7.5 mm. It can be seen that the measured and simulated reflection losses and reflection phases agree fairly well. Referring to Figure 4(a), two dips are spotted at $R_2 = 4.7$ mm and $R_2 = 5.7$ mm with reflection loss not larger than -0.9 dB in measurement. This shows that the proposed unit element has very low loss at all patch dimensions, which is helpful for increasing radiation efficiency of the reflectarray. Figure 4(b) shows the measured and simulated reflection phases. With reference to the figure, a gradual decreasing phase slope with a total reflection phase range of 681.82° has successfully been achieved. Although the phase linearity of the parallel print dipoles [14] appears to be better, the proposed multilayer structure here can posssibly offer a compact footprint if more elements are needed for an even larger phase range. Having a large phase range exceeding 360° implies that the proposed unit element can be used to design large-size reflectarrays.

To further understand the patch resonances that enable such a broad phase range, the electric field distributions between the top and middle patches as well as that formed between middle patch and ground are studied for the cases $R_1 = R_2 = 4.7$ mm and 5.7 mm, shown in Figure 5. Comparing Figures 5(a) and (c), it is obvious that the two resonances are the TM^z_{110} mode of the circular microstrip patch resonator [23]. It simply means that this resonance is excitable in the double-layered structure at these two radii. The frequency response is then studied. Figure 6 shows the measured and simulated reflection coefficients and reflection angles of the proposed unit element for the dimension of $R_1 = R_2 = 6.1$ mm. Good agreement has been found between the measured and simulated results. With

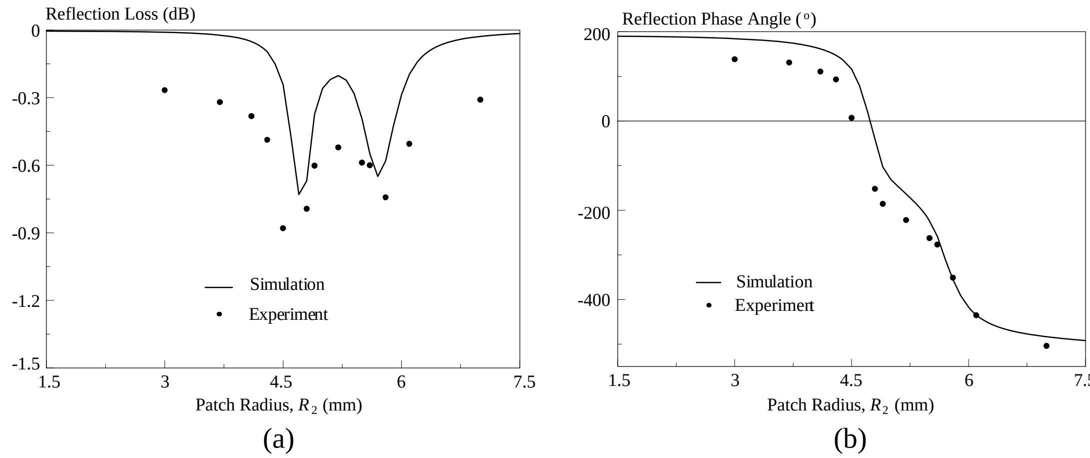

Figure 4. Measured and simulated (a) reflection losses, (b) reflection phase angles of the proposed double-layered reflectarray unit element.

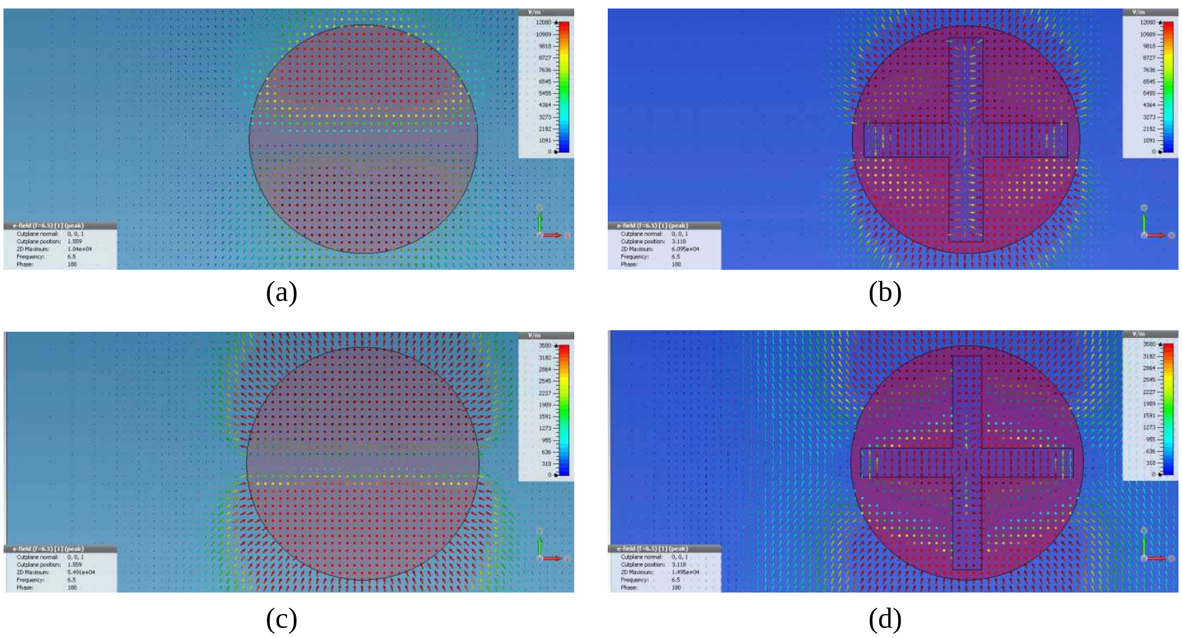

Figure 5. Electric field distributions between (a) middle patch and ground at $R_1 = R_2 = 4.7\,\text{mm}$, (b) top and middle patch at $R_1 = R_2 = 4.7\,\text{mm}$, (c) middle patch and ground at $R_1 = R_2 = 5.7\,\text{mm}$, (d) top and middle patch at $R_1 = R_2 = 5.7\,\text{mm}$.

reference to Figure 6(a), it is obvious that the measured and simulated curves are in the same trend, with slight discrepancy. The additional $\sim$0.5 dB loss in measurement can be introduced by the SMA connector (shown in Figure 3), which is not accounted for in simulation. With reference to Figure 6(b), the discrepancy between the measured and simulated reflection phase is not larger than 0.5%, which is acceptable.

Parametric analysis has also been performed using the waveguide model. First, the effect of the radius of the middle patch (R_2) is studied. With reference to Figure 7, the radius of the top circular patch (R_1) is varied from 1.5 to 7.5 mm. Regardless of the value of R_2, as can be seen from Figure 7(a), the double-layered structure has its resonant frequency of around 6.5 GHz when R_1 approaches $\sim$4.7 mm, which can be justified from the loss performance. Higher loss is induced as the radius of the middle circular patch becomes larger. Steeper phase slope is obtainable by increasing the radius of the middle

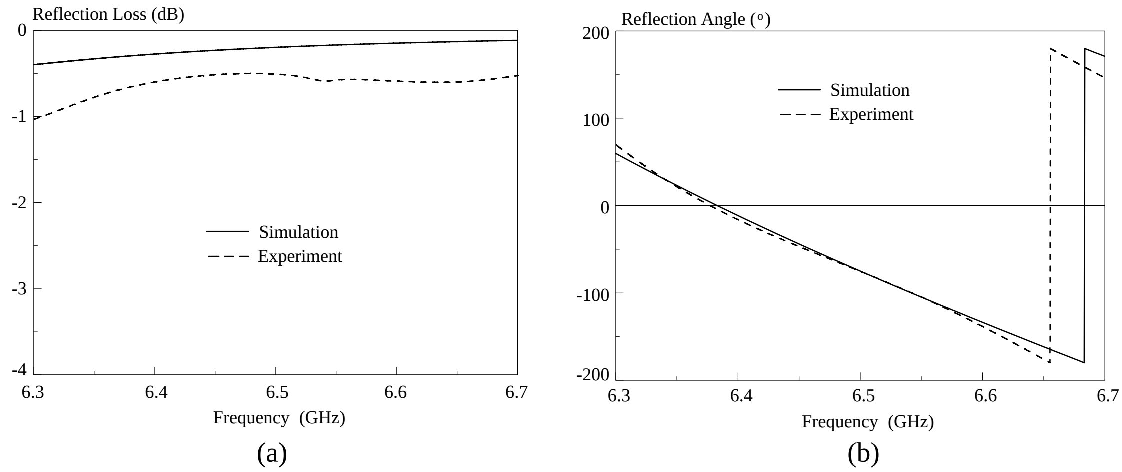

Figure 6. Measured and simulated (a) reflection coefficients, (b) angles of reflection against frequency for $R_1 = R_2 = 6.1\,\mathrm{mm}$ of the proposed double-layered reflectarray unit element.

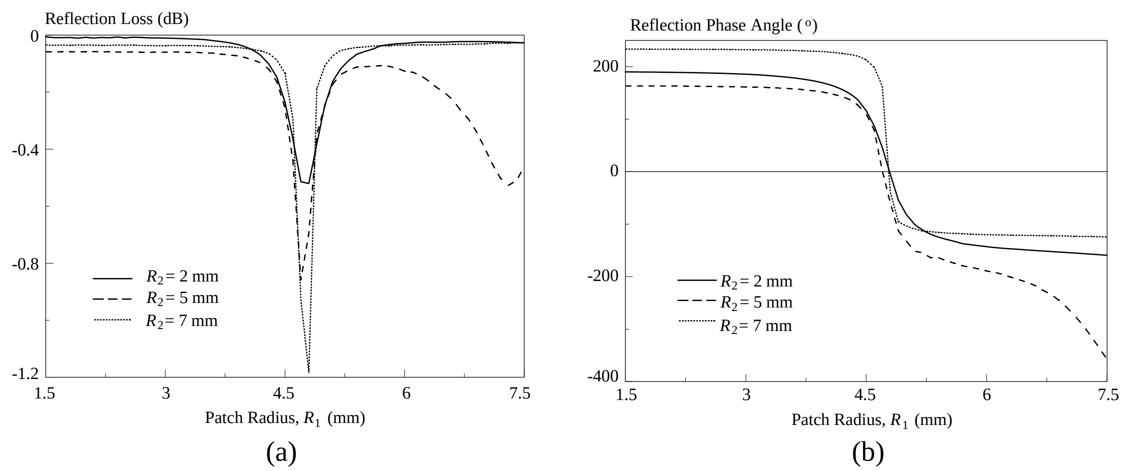

Figure 7. Effects of the middle circular patch radius (R_2) on the (a) reflection loss; (b) reflection phase angle of the proposed double-layered reflectarray unit element.

circular patch from 2 to 7 mm, as can be observed in Figure 7(b). Also referring to the same figure, it is noted that a patch with $R_2 = 5\,\mathrm{mm}$ has a much greater reflection phase range than other two ($R_2 = 2\,\mathrm{mm}$ and 7 mm). The effect of radius difference ($d_1 = R_2 - R_1$), where the two patches are varied at the same time and $R_2 > R_1$, is now studied. Figure 8(a) compares the reflection losses for different d_1. Referring to the curves in Figure 8(b), it can be seen that the slope changing rate can be tuned by creating a radius difference in the top and middle patches. For all cases, the phase ranges are greater than 650°. Abrupt gradient change should be avoided.

Next, the effects of changing slot widths and lengths are studied. In the first study, the widths of the horizontal (W_1) and vertical (W_2) slots are varied concurrently, with $R_1 = R_2$. With reference to Figure 9(a), for all three cases, their maximum reflection losses can be kept well below $-1.2\,\mathrm{dB}$. With reference to Figure 9(b), the slope change of the reflection phase becomes slower with increasing slot widths (W_1, W_2), which is much desired as it makes the unit elements more distinguishable in dimension. It should also be mentioned that varying the slot widths (W_1, W_2) at the same time does not degrade the phase range. In the second study, the lengths of the horizontal (L_1) and vertical (L_2) slots are varied simultaneously and the results are shown in Figure 10. Again, $R_1 = R_2$. In Figure 10(a), it is observed that longer slots introduce higher loss. With reference to Figure 10(b), varying the slot lengths (L_1, L_2) will only affect the gradient of the reflection phase angle when the patch radius (R_2) is more than 6 mm. Also observed is that the phase change becomes faster with increasing reflection loss.

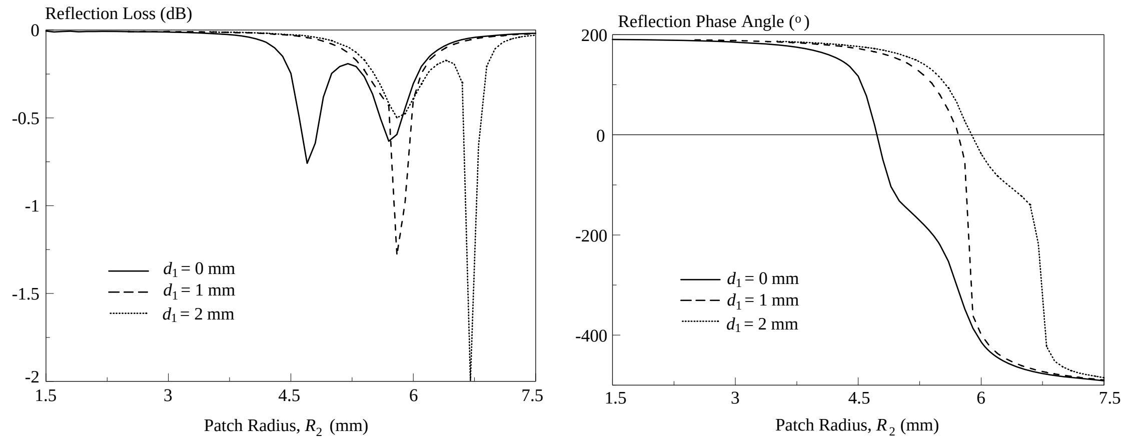

(a) (b)

Figure 8. Effects of the radius difference d_1 (where $R_2 > R_1$) on the (a) reflection loss; (b) reflection phase angle of the proposed double-layered reflectarray unit element.

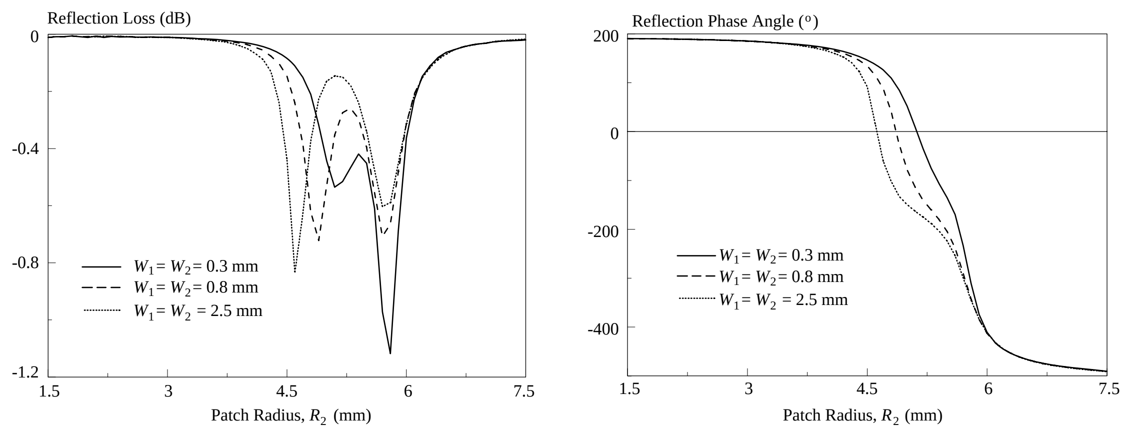

(a) (b)

Figure 9. Effects of the slot widths (W_1, W_2) on the (a) reflection loss; (b) reflection phase angle of the proposed double-layered reflectarray unit element.

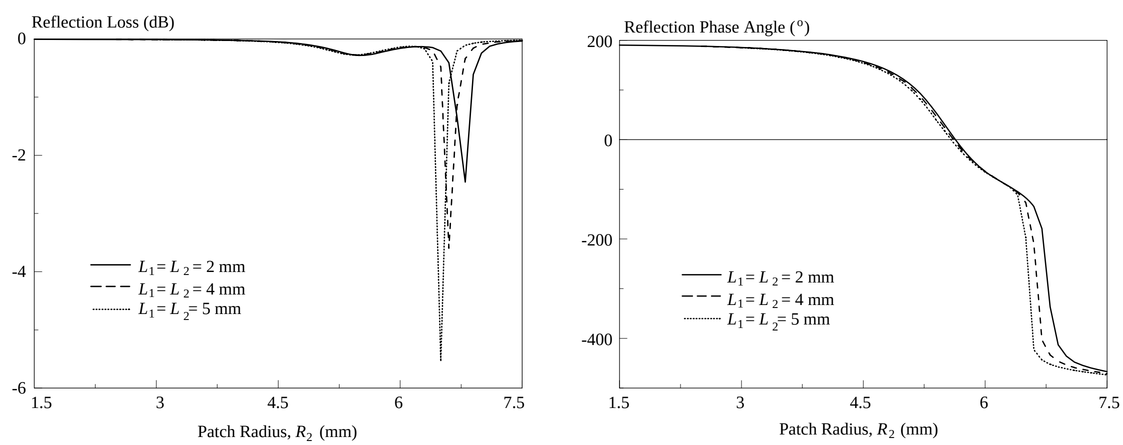

(a) (b)

Figure 10. Effects of the slot lengths (L_1, L_2) on the (a) reflection loss; (b) reflection phase angle of the proposed double-layered reflectarray unit element.

To study the effects of the substrates on the reflection characteristics, different sets of substrates (Substrate 1 and 2) with the same dielectric constant (ε_r) are simulated, with $R_1 = R_2$. Referring to Figure 11(a), a slightly higher reflection loss which has a peak at -1.4 dB, when the patch radius $R_2 = 4.1$ mm, is observed if substrates with dielectric constant of 6.15 are used. The other two sets of substrates ($\varepsilon_r = 2$ and 3.38) have a maximum reflection loss of $\sim$$-0.7$ dB, with both values close even though they are designed with different patch radii R_2. Again, it can be noted that using a substrate with higher dielectric constant (ε_r) value causes the unit element to resonate at a smaller patch radius of R_2. The reflection phase characteristics shown in Figure 11(b) demonstrate that the slope gradient can be easily tuned without affecting the phase range.

Next, unit elements with different combinations of top and middle patches are explored and their reflection characteristics are studied in Figure 12. Again, the patches are set to have equal radius ($R_2 = R_1$) and the slots are defined as $W_1 = W_2 = 1.4$ mm and $L_1 = L_2 = 2 \times (R_1 - 0.5)$. Referring to Figure 12(a), the reflection loss for the unit element with either its top or middle patch etched with a slot is shown to be able to be kept well below -1 dB. The unit element with both of its top and middle patches containing slots has the highest reflection loss, peaking at $\sim$$-4.2$ dB. The reflection phase angle is then studied in Figure 12(b). Comparing all four combinations, it can be seen that unit element with only its top patch etched has the largest phase range, giving reasonably slow reflection phase slope. Rapid change in gradient is observed in the unit element that has only its middle patch etched, which should be avoided when designing a reflectarray. Also, it is noted that the unit element with slots etched

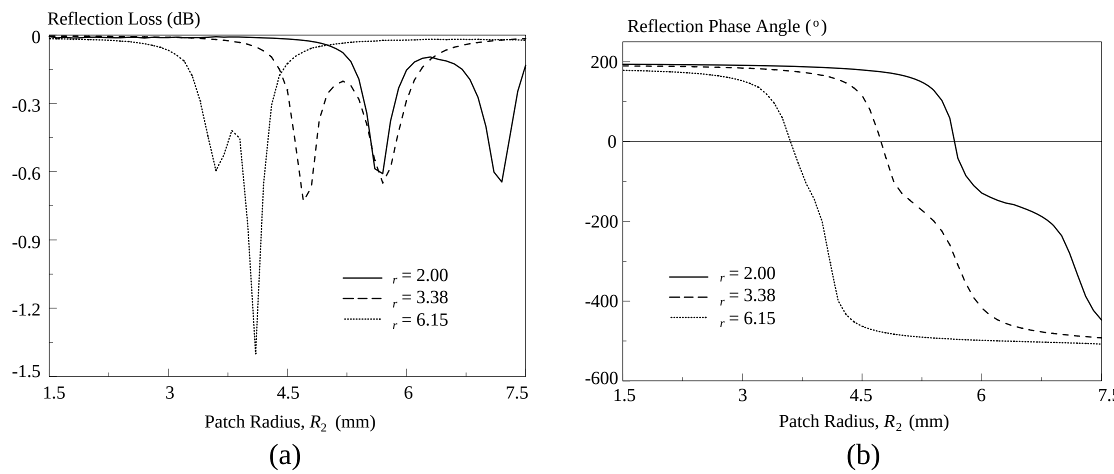

Figure 11. Effects of the substrate dielectric constant ε_r on the (a) reflection loss; (b) reflection phase angle of the proposed double-layered reflectarray unit element.

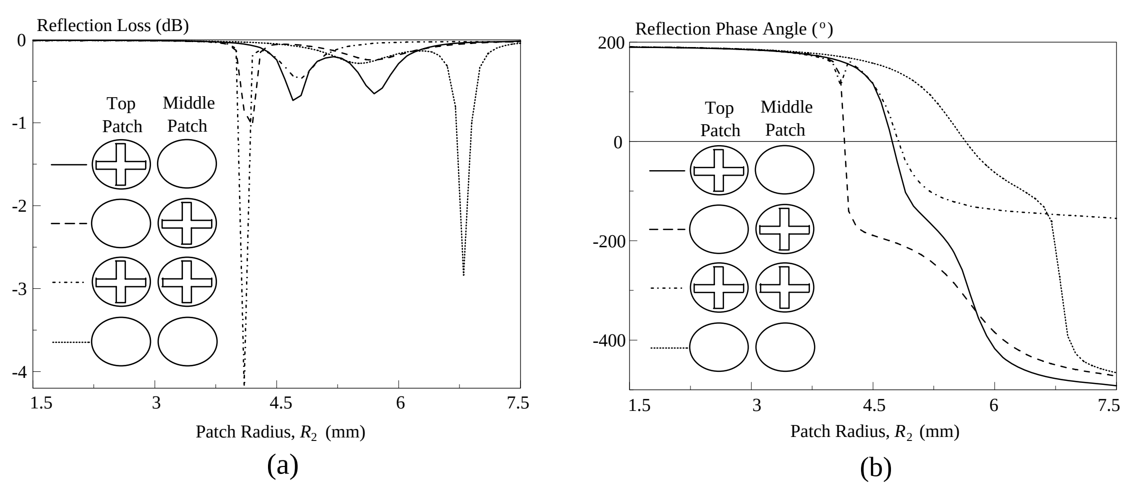

Figure 12. Different combinations of top and middle circular patches on the (a) reflection loss; (b) reflection phase angle.

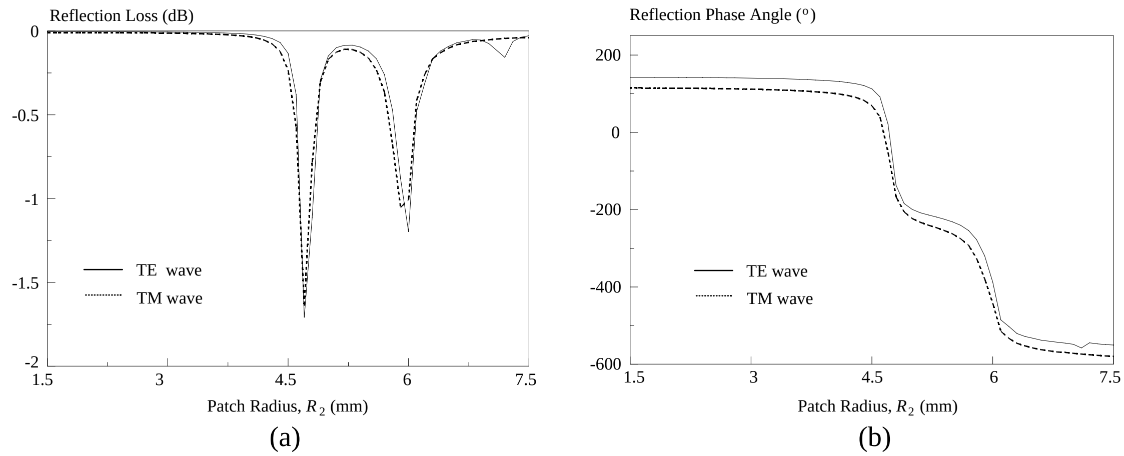

Figure 13. (a) Reflection losses and (b) reflection phase angles for the TE- and TM-polarized incoming waves.

on both patches is unable to provide phase range of more than 400°, although gradual phase slope is achievable.

With the use of Floquet model ($h = 154\,\mathrm{mm}$, $l_1 = l_2 \approx 0.5\lambda$), the electric field polarization is now studied for an incident wave coming from the direction of $\phi = -90^\circ$ and $\theta = 48.58^\circ$, where y-z plane is the incident plane. The elevation angle of $\theta = 48.58^\circ$ is selected so that the result can be compared with that of the waveguide model, which also has an incident angle of $\alpha = 48.58^\circ$ at 6.5 GHz. Here, an incident wave with its electric field perpendicular to the incident plane is defined to be the Transverse-Electric-Field (TE) wave; while the case for an incoming wave with its magnetic field normal to this plane is called Transverse-Magnetic-Field (TM) wave. Figure 13 shows the simulated reflection losses and reflection phase angles for the TE and TM incident waves. It is obvious that the two cases have almost the same characteristics due to the symmetry of the element structure in the x- and y-directions.

4. CONCLUSIONS

In this paper, a double-layered microstrip reflectarray element with broad phase range has been proposed. A reflection phase range of 681.82° with low reflection loss ($< -1\,\mathrm{dB}$) is achievable. The effects of the patches, slots, and substrates of the unit element on the reflection characteristics have also been investigated. It has been found that the phase range can be manipulated by adjusting the top and middle circular patch radii. Also, the changing rate of the reflection phase slope can be altered in several ways, namely, changing the slot widths simultaneously, adjusting the radius difference between two circular patches, and using substrates with different dielectric constants. Good agreement has been found between the simulated and experimental data.

ACKNOWLEDGMENT

The work described in this paper was supported by a Science Fund (Project No. 06-02-11-SF0087) funded by the Ministry of Science, Technology and Innovation, Malaysia. Part of the project is also sponsored by an UTAR Research Fund 2013 (Project No. 6200/LA5).

REFERENCES

1. Huang, J. and J. A. Encinar, *Reflectarray Antenna*, John Wiley & Sons, Inc., Hoboken, 2007.
2. Berry, D., R. Malech, and W. Kennedy, "The reflectarray antenna," *IEEE Trans. Antennas Propag.*, Vol. 11, No. 6, 645–651, Nov. 1963.
3. Huang, J., "Microstrip reflectarray," *IEEE Intl. Symp. Antennas Propagat.*, Vol. 2, 612–615, Jun. 1991.

4. Pozar, D. M., S. D. Targonski, and H. D. Syrigos, "Design of millimeter wave microstrip reflectarrays," *IEEE Trans. Antennas Propagat.*, Vol. 45, No. 2, 287–296, Feb. 1997.
5. Gonzalez, D. G., G. E. Pollon, and J. F. Walker, "Microwave phasing structures for electromagnetically emulating reflective surfaces and focusing elements of selected geometry," US Patent 4905014, 1990.
6. Encinar, J. A., "Design of two-layer printed reflectarray using patches of variable size," *IEEE Trans. Antennas Propagat.*, Vol. 49, No. 10, 1403–1410, Oct. 2001.
7. Huang, J., "Microstrip reflectarray," *IEEE Intl. Symp. Antennas Propagat.*, 612–615, Ontario, Canada, Jun. 1991.
8. Carrasco, E., M. Barba, and J. A. Encinar, "Reflectarray element based on aperture-coupled patches with slots and lines of variable length," *IEEE Trans. Antennas Propagat.*, Vol. 55, No. 3, 820–825, Mar. 2007.
9. Hasani, H., M. Kamyab, and A. Mirkamali, "Broadband reflectarray antenna incorporating disk elements with attached phase-delay lines," *IEEE Antennas Wireless Propagat. Lett.*, Vol. 9, 156–158, 2010.
10. Huang, J. and R. J. Pogorzelski, "A Ka-band microstrip reflectarray with elements having variable rotation angles," *IEEE Trans. Antennas Propagat.*, Vol. 46, No. 5, 650–656, May 1998.
11. Oh, S. W., C. H. Ahn, and K. Chang, "Reflectarray element using variable ring with slot on ground plane," *Electron. Lett.*, Vol. 45, No. 24, 1206–1207, Nov. 2009.
12. Chaharmir, M. R., J. Shaker, M. Cuhaci, and A. Sebak, "Reflectarray with variable slots on ground plane," *IEEE Proceedings Microw., Antennas and Propagat.*, Vol. 150, No. 6, 436–439, Dec. 2003.
13. Maddahali, M. and K. Forooraghi, "High efficiency reflectarray using smooth tapering in phase pattern on antenna surface," *Microw. Opt. Technol. Lett.*, Vol. 55, No. 4, 747–753, Apr. 2013.
14. Florencio, R., R. R. Boix, E. Carrasco, J. A. Encinar, M. Barba, and G. P. Palomino, "Broadband reflectarrays made of cells with three coplanar parallel dipoles," *Microw. Opt. Technol. Lett.*, Vol. 56, No. 3, 748–753, Mar. 2014.
15. Chaharmir, M. R., J. Shaker, M. Cuhaci, and A. Ittipiboon, "A broadband reflectarray antenna with double square rings," *Microw. Opt. Technol. Lett.*, Vol. 48, No. 7, 1317–1320, Jul. 2006.
16. Li, Y., M. E. Bialkowski, K. H. Sayidmarie, and N. V. Shuley, "Microstrip reflectarray formed by double elliptical ring elements," *Proceedings of the Fourth European Conf. on Antennas and Propagat.*, 1–5, Apr. 2010.
17. Chaharmir, M. R., J. Shaker, N. Gagnon, and D. Lee, "Design of broadband, single layer dual-band large reflectarray using multi open loop elements," *IEEE Trans. Antennas Propag.*, Vol. 58, No. 9, 2875–2883, Sep. 2010.
18. Maruyama, T., T. Furuno, Y. Oda, J. Shen, and T. Ohya, "Analysis and design of metamaterial reflectarray using combination of multilayer mushroom-structure," *IEEE Intl. Symp. Antennas Propagat.*, 1–4, Jul. 2010.
19. Maruyama, T., T. Furuno, Y. Oda, J. Shen, and T. Ohya, "Capacitance value control for metamaterial reflectarray using multi layer mushroom-structure with parasitic element," *IEEE Intl. Conf. Wireless Information Tech. Systems*, 1–4, Sep. 2010.
20. Maruyama, T., T. Furuno, Y. Oda, J. Shen, N. Tran, and H. Kayama, "Design of wide angle reflection reflectarray using multi-layer mushroom structure to improve propagation," *XXXth URSI General Assembly and Scientific Symp.*, 1–4, Aug. 2011.
21. Carrasco, E., M. Barba, and J. A. Encinar, "Reflectarray element based on aperture-coupled patches with slots and lines of variable length," *IEEE Trans. Antennas Propagat.*, Vol. 55, No. 3, 820–825, Mar. 2007.
22. Dzulkipli, I., H. H. Jamaluddin, R. Gillard, R. Sauleau, R. Ngah, M. R. Kamarudin, N. Seman, and M. K. A. Rahim, "Mutual coupling analysis using FDTD for dielectric resonator antenna reflectarray radiation prediction," *Progress In Electromagnetics Research B*, Vol. 41, 121–136, 2012.
23. Ng, W. H., E. H. Lim, F. L. Lo, and K. H. Tan, "Study of cross-slotted circular microstrip for reflectarray design," *Progress In Electromagnetics Research C*, Vol. 50, 11–19, 2014.